Academic Platform Journal of Engineering and Science

journal homepage: http://apjes.com/

Theoretical and Experimental Investigation of Carbon Monoxide, Humidity and Temperature Relations in Zonguldak Province of Turkey

Caglar Celik Bayar

Zonguldak Bulent Ecevit University, Department of Metallurgical and Materials Engineering, 67100 Zonguldak/Turkey,

caglarbayar@gmail.com, caglarbayar@beun.edu.tr, iD

Abstract

The sensor monitoring of ambient carbon monoxide (CO) which was mainly emitted by the coal mines and power plants was performed in the center of Zonguldak province of Turkey. It was observed that the recorded amount of CO (ppm) highly depended on the amount of humidity (H_2O) percent and temperature. The sensor monitored higher CO values at higher temperatures accompanied with lower humidity percent whereas lower CO values at lower temperatures accompanied with higher humidity percent. Consequently, $OC\ldots W_n$ (W: H_2O) (n = 1-3) long-range (hydrogen-bonding) interactions were modelled computationally using MP2/6-311++G(d,p) level of theory at selected temperatures. The calculated interaction Gibbs free energies and performed reactivity and stability analyses supported the possibility of carbon monoxide and humidity interactions at lower temperatures with higher humidity percent in parallel with the experimental results. It was concluded that the system presented in this study might be integrated into CO sensor units to improve the sensor response in terms of accuracy and precision.

Keywords: carbon monoxide, humidity, sensor monitoring, computational modeling, MP2

1. INTRODUCTION

The present study includes the monitoring of CO gas with sensors and modeling of its possible interactions with water (humidity) molecules. Therefore, the types of sensors and their characteristics, the general properties of CO gas and its effects on our health and the previous studies about CO-water interactions reported in the literature were presented at the beginning of this section.

Air pollution is one of the main causes of acute and chronic diseases. The pollutants in the atmosphere are predominantly particles and gases such as nitrogen dioxide (NO_2), ozone (O_3) and carbon monoxide (CO) [1]. Compact, low-cost and portable gas sensors are highly preferable in the field of ambient air quality monitoring [1-4]. These sensors have different working principles according to their types. For instance, photo-ionization based sensors are generally used for detecting volatile organic compounds [1,5]. Carbon dioxide (CO_2) and methane (CH_4) gases can be detected by optical sensors which are based on measuring gas absorption at a specific infrared wavelength [1,6]. Semi conductive metal oxide sensors work on the basis of changes in conductivity when they are in contact with pollutant gas molecules [1,7]. Oxidation/reduction reactions that occur on the electrodes of electrochemical sensors result in change in current and help in detecting several of the gas pollutants [1,8,9]. However, the data quality of sensor monitoring is highly affected from environmental factors such as temperature, humidity and interference of other air pollutants

[1,4,8,10]. Machine learning methods are used and still in progress in order to overcome these problems.

CO is an important air pollutant. It is a gas with no color, odor and taste. It is predominantly produced from the incomplete combustion of fossil fuels. The other sources of CO are natural gas, volcanoes, open fires and metabolism of marine organisms. It is a toxic gas. As hemoglobin (Hb) (the oxygen transport protein contained in the red blood cells) has about 220 times more affinity for CO than it does for oxygen, a rapid poisoning of red blood cells occurs when the body is exposed to a high concentration of CO. The COHb concentration should not exceed a recommended universal level of 2.5%. High levels of CO exposure can cause acute poisoning, leading the coma and death at COHb levels of greater than 40% [11].

Atmospheric CO level is highly affected by the amount of humidity. There exist different studies on this subject in the literature. The $OC\ldots H_2O$ complex was firstly observed experimentally in solid argon [12]. Rotational transitions for this structure and its different isotopic versions were investigated using the molecular beam electric resonance and Fourier transform microwave absorption techniques [13]. The combination of the supermolecular Møller-Plesset scheme with the perturbation theory of intermolecular forces was applied in the analysis of the potential energy surface of $OC\ldots H_2O$ [14]. Additionally, various density functional methods and local and nonlocal exchange-correlation functionals were used in the investigation of the structure,

*Corresponding Author: Zonguldak Bulent Ecevit University, Department of Metallurgical and Materials Engineering, 67100 Zonguldak/Turkey, caglarbayar@gmail.com, caglarbayar@beun.edu.tr

energetics and vibrational properties of the same complex [15].

The present study was performed in Zonguldak province of Turkey. It is located in the western Black Sea region of the country. The specific geographic property of Zonguldak center is that the transition between the temperatures in the winter months is soft while that of the humidity percentages are quite hard. It is a major mining center of Turkey and CO emissions from the coal mines to the atmosphere reach very high values. In addition, there are many power plants near the city center which use coal as a fuel and release a significant amount of CO into the environment. These CO emissions pose a serious threat to the city and therefore need to be measured correctly. In a region with such characteristics, first the humidity and then the temperature as a humidity drier were considered to be very important factors on carbon monoxide sensors. In this perspective, the relationship between CO level-humidity and CO level-temperature were examined by sensor monitoring in February in Zonguldak center. The month of February was chosen for collecting experimental data because of hard humidity percent transitions in winter months. The experimental records were then computationally modeled taking into account long-range interactions of carbon monoxide and humidity at selected temperatures which were demonstrated as $OC...W_n$ throughout the study (OC: Carbon monoxide interacting from carbon side, W: H_2O: Humidity, n = 1-3). The previous studies mostly focused on structural

analysis of $OC...H_2O$ complex as mentioned earlier. Such a study consisting of both sensor monitoring and computational modeling of CO-humidity interactions does not exist in the literature. Thus, the originality of the study is revealed.

2. MATERIALS AND METHOD

2.1. Experimental Monitoring

The experimental setup included a semi conductive metal oxide CO sensor with MQ-7 brand (Figure 1) to record atmospheric CO levels in ppm and a BME280 branded sensor (Figure 2) to record pressure (hPa), temperature ($^\circ$C) and humidity (%) changes. Data coming from these sensors were decoded by the use of a 10-bits Atmel based microprocessor. An Ethernet shield was coupled with the microprocessor (Figure 3) to save the real time data coming from these sensors into a SD card. Note that Figures 1-3 show the original pictures of the purchased items. The working frequency of the experimental setup was adjusted to 1 Hz. The sensor data was collected for a week without any interruptions. C-Based programming language was used to create algorithms. Open source libraries provided by the manufacturers of the sensors were integrated into the program.

MQ-7 branded sensor is often used to detect CO levels in industry and car automation setups. It works with 5V DC

Figure 1. The picture of a semi conductive metal oxide CO sensor with MQ-7 brand.

Figure 2. The picture of a BME280 branded pressure-temperature-humidity sensor.

Figure 3. The picture of microprocessor (bottom component) and Ethernet shield (top component) together.

voltage and sends its data by analog resistance. The detecting range is between 20 ppm-2000 ppm CO. The sensitivity of the load resistance is 10 kΩ ±5%.

BME280, manufactured by Bosch, is an environmental sensor. It provides temperature, barometric pressure and humidity information. Sharp changes of environmental conditions and weather/environmental sensing can be monitored using this sensor. It has the capability of communicating with the microprocessor over I2C or SPI (I2C communication protocol was used to get fast and accurate conversion in the experimental setup). This low-

cost sensor can measure humidity with ±3% accuracy. Temperature and barometric pressure can be sensed with the accuracies of ±1°C and ±1 hPa, respectively. It needs 5V DC power to work. It was programmed to send its data in each second in the experimental setup.

The graphs of time versus recorded temperature, pressure, humidity and CO level were presented in Figure 4. It was detected that the atmospheric pressure almost stayed at around 1.00 atm. during the measurements when the recorded pressures in hPa were converted to atm. Therefore, pressure was not taken as a variable, was considered as a

constant, both in experimental monitoring and computational modeling. The data collected all fluctuated in Figure 4 which denoted a reasonable time interval was needed to reach equilibrium and obtain more reliable results. Table 1 presented the minimum, intermediate and maximum CO levels and other related values obtained from Figure 4. The data in Table 1 was interpreted like this: At the minute of 100 the minimum CO level was measured as 30 ppm at 6 °C with the atmospheric humidity of 68 %. Approximately 8 hours later (at the minute of 600), the temperature increased to 11 °C and dried the humidity to 54 %. The level of free atmospheric CO increased to 55 ppm with decrease in humidity. Then, approximately 6 hours later, at the minute of 980, the temperature increased to 14 °C and dried the humidity some more (52 %). At that point the free CO level reached its maximum value of 75 ppm. Another interpretation was like that: The increase of temperature from 6 to 11 °C ($\Delta t = 5$ °C) dried the humidity level 14 % and increased the free CO level 25 ppm. However, when the temperature increased from 11 to 14 °C ($\Delta t = 3$ °C), the humidity decreased 2% that resulted in 20 ppm increase in CO level. After these observations it was concluded that the amount of change in temperature (Δt) was an important factor in determining the humidity % and free CO levels. Regarding to that, in the cases of 6 and 14 °C in which Δt was 8 °C, humidity decrease was 16 % and increase in CO level was 45 ppm. These observations brought to mind that chemical interactions might take place between CO and humidity (H_2O) molecules at lower temperatures accompanying with higher humidity. This was the main approach used in the computational modeling.

2.2. Computational Modeling

The interactions of CO gas with one, two and tree water (humidity) molecules were modeled computationally. They were abbreviated as OC…W (CO molecule was interacting with one water molecule from carbon side), OC…W…W (OC…2W) (CO molecule was interacting with one water molecule from carbon side and the water molecule was interacting with another water molecule), OC…W…W…W (OC…3W) (similar to the previous one but there were three water molecules interacting with each other). All interactions were detected as long-range (hydrogen-bonding) interactions after calculations.

The initial structure optimizations leading to the energy minima were performed using the MM2 method followed by the semi-empirical PM3 self-consistent field molecular orbital (SCF-MO) method [16] and Hartree-Fock (HF) SCF-MO methods [17] at the restricted level. Further optimizations were performed within the framework of Second-order Moller-Plesset Perturbation Theory (MP2) at the restricted level of a 6-311++G(d,p) basis set (MP2/6-311++G(d,p)) [17]. All vibrational analyses and thermochemical calculations were performed using the same level of theory. The vibrational analyses had no imaginary
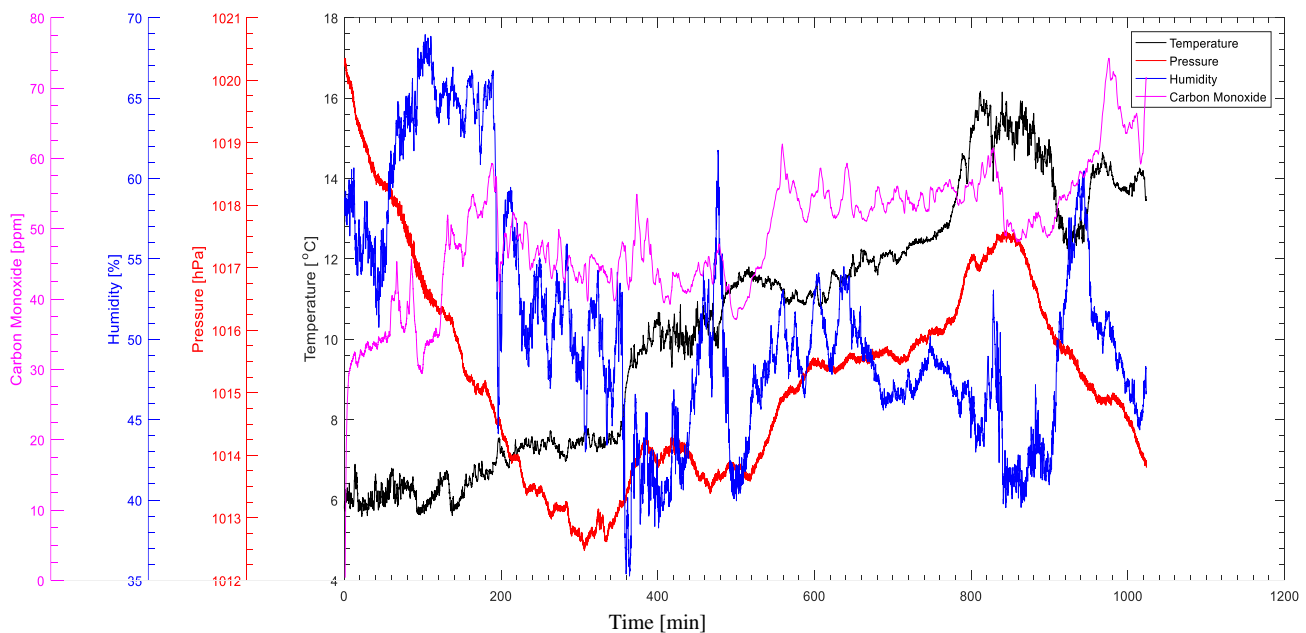
Figure 4. The graphs of time versus temperature (°C), pressure (hPa), humidity (%) and CO level (ppm).

Table 1. The minimum, intermediate and maximum CO levels and other related values obtained from Figure 4.

Time (min)	Temperature (^{o}C)	Free CO (ppm)	Humidity (%)
100	6	30[a]	68
600	11	55[b]	54
980	14	75[c]	52
[a,c]The minimum and maximum values of CO recorded in time interval of approximately 15 hours. [b]An intermediate value of CO recorded approximately after 8 hours than the first measurement. Atmospheric pressure was at around 1.00 atm.			

frequencies, which indicated that no transition states or saddle points were observed on the potential energy surfaces. The interaction Gibbs free energies of all the considered long-range interactions were calculated at 6, 11 and 14 ^{o}C, respectively. Then, they were corrected with basis set superposition error (BSSE) contributions [18,19]. BSSE corrections use the Boys and Bernardi counterpoise technique [18,20], which are due to overlap of the wave functions of the moieties [21]. All of the computations were performed for the gas phase using the Gaussian 09 software package [22]. The atmospheric pressure was kept at 1.00 atm. during calculations.

3. RESULTS AND DISCUSSION

3.1. Structure Optimizations

In OC…W (OC…H_2O) structure, the hydrogen bond between the two fragments, CO and H_2O (OC…H-O-H), was determined to be 2.41 Å with nonlinearity of 11.5^o in the literature [12,15]. Additionally, the higher stability of OC…W interaction rather than CO…W interaction was reported computationally [14] (Long-range interaction was from the C side in the previous structure, however it was from the O side in the latter). Similarly, the present study concentrated on the stable OC…W structure. The values calculated in the study were close to the ones reported in the literature. The hydrogen bond length in OC…W structure was found to be 2.45 Å accompanied by a nonlinearity of 10.8^o at all temperatures.

The shapes of the optimized structures were similar at all temperatures of 6, 11 and 14 ^{o}C. Therefore, the representative temperature was chosen as 6 ^{o}C and the optimized structures of OC…W, OC…2W and OC…3W interactions were demonstrated at this temperature in Figure 5. All interactions had OC…H-O-H hydrogen bonds. In OC…2W and OC…3W interactions, water molecules were oriented to make additional hydrogen bonds between them.

Interaction		
OC…W	OC…2W	OC…3W
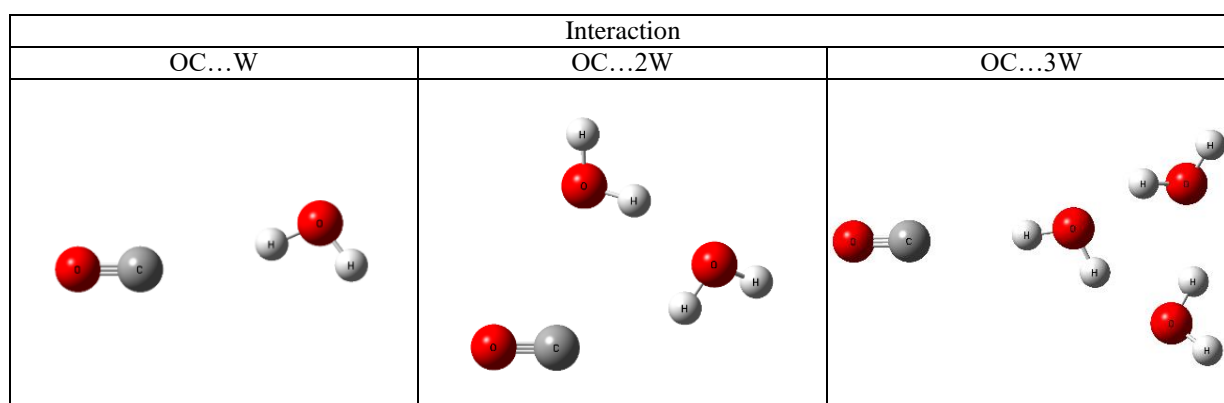
Figure 5. The representative optimized structures of OC…W, OC…2W and OC…3W interactions at the theoretical level of MP2/6-311++G(d,p) at 6 ^{o}C.

3.2. Computed Interaction Gibbs Free Energies and Relation with Sensor Monitoring

The interaction Gibbs free energies were formulated as in Equation (1):

$$\Delta G_{int}^o = \Delta G^o(OC \ldots W_n) - [\Delta G^o(CO) + n\,\Delta G^o(W)] ,$$
$$n = 1 - 3 \tag{1}$$

The BSSE corrected interaction Gibbs free energies of all the considered interactions were presented in Table 2. The following results were obtained from calculations: At any selected temperature the interaction Gibbs free energy was positive (non-spontaneous) and the energy order was OC…3W > OC…2W > OC…W. It denoted that the interaction got more difficult with increasing number of water. If the amount of water was increased from 1 mole to 2 moles (W was added to OC…W and OC…2W was

formed), an additional energy more than 20 kJ/mole was needed to perform the reaction at any temperature. However, when the mole number of water molecules were increased from 2 to 3, less energy was needed (3-4 kJ/mole) (W was added to OC…2W and OC…3W was formed at any temperature). Additionally, it needed more energy to perform OC…W$_n$ interaction (n = 1-3) as temperature increased. This observation was parallel to the sensor monitoring result in which the concentration of free CO (non-bonding CO) increased with increasing temperature (with drying humidity).

3.3. The Frontier Molecular Orbital Analyses

The frontier molecular orbital analyses of the structures were performed using the orbitals of HOMO (Highest Occupied Molecular Orbital) and LUMO (Lowest Unoccupied Molecular Orbital). Absolute hardness (η), global softness (S), Mulliken electronegativity (X_M), electronic chemical potential (μ), electrophilicity index (ω) and $f_{H/L}$ index are important parameters to understand the chemical reactivity

and stability of the compounds. They are calculated by the Equations (2)-(6) given below.

$$\eta = \frac{(I - A)}{2} \quad [23,24] \tag{2}$$

$$S = \frac{1}{(2\eta)} \quad [24,25] \tag{3}$$

$$X_M = -\mu = \frac{(I + A)}{2} \quad [23,25] \tag{4}$$

$$\omega = \frac{\mu^2}{(2\eta)} \quad [25,26] \tag{5}$$

$$f_{H/L} = \frac{\varepsilon_{HOMO}}{\varepsilon_{LUMO}} \quad [27] \tag{6}$$

I and A are the ionization potential and electron affinity, respectively [23]. Note that $I = -\varepsilon_{HOMO}$ and $A = -\varepsilon_{LUMO}$ within the validity of the Koopmans' theorem [28], where ε_{HOMO} and ε_{LUMO} are the energies of the highest occupied molecular orbital and lowest unoccupied molecular orbital, respectively.

The calculated frontier molecular orbital energies and related reactivity and stability parameters of CO, W and OC…W$_n$ (n = 1-3) structures at the theoretical level of MP2/6-311++G(d,p) were demonstrated in Table 3. According to the results it was concluded that W had a tendency to interact with CO as their absolute hardness and global softness values were close to each other. CO was a little bit harder than W ($\eta_{CO} = 0.32\ eV$, $\eta_W = 0.28\ eV$) and in parallel W was a little bit softer than CO ($S_W = 1.79\ eV^{-1}$, $S_{CO} = 1.56\ eV^{-1}$). It is important to note that hard-hard (soft-soft) interactions have more tendency to occur chemically than hard-soft interactions [29,30]. In this perspective, the interaction of OC…W with another W molecule (to form OC…2W) was also favored since the absolute hardness and

Table 2. Calculated interaction Gibbs free energies of CO molecule with different numbers of water molecule (humidity) at the selected temperatures. MP2/6-311++G(d,p) theoretical level was used in the calculations.

Interaction			
Temperature	OC…W	OC…2W	OC…3W
6	19.1	40.4	43.5
11	19.5	41.5	45.1
14	19.7	42.1	46.1

Temperatures are in °C.
Energies are standard Gibbs free energies in kJ/mole and BSSE corrected.
Atmospheric pressure was fixed at 1.00 atm. in computations.

Table 3. The calculated frontier molecular orbital energies and related reactivity and stability parameters of CO, W (water) and OC…W$_n$ (n = 1-3) structures at the theoretical level of MP2/6-311++G(d,p).

	ε_{HOMO} (eV)	ε_{LUMO} (eV)	I (eV)	A (eV)	η (eV)	S (eV^{-1})	$X_{M = -\mu}$ (eV)	ω (eV)	$f_{H/L}$
CO	-0.56	0.083	0.56	-0.083	0.32	1.56	0.24	0.090	-6.75
W	-0.51	0.043	0.51	-0.043	0.28	1.79	0.23	0.094	-11.86
OC…W	-0.50	0.050	0.50	-0.050	0.28	1.79	0.23	0.094	-10.00
OC…2W	-0.49	0.042	0.49	-0.042	0.27	1.85	0.22	0.090	-11.67
OC…3W	-0.50	0.045	0.50	-0.045	0.27	1.85	0.23	0.098	-11.11

global softness values of OC…W and W were the same ($\eta = 0.28\ eV$, $S = 1.79\ eV^{-1}$ for both). Similarly, the interaction

of OC…2W with another W molecule (to form OC…3W) was possible when their closer η and S values were taken

into account ($\eta_W = 0.28\ eV, \eta_{OC\ldots 2W} = 0.27\ eV,\ S_W = 1.79\ eV^{-1}, S_{OC\ldots 2W} = 1.85\ eV^{-1}$).

Electrophilicity index (ω) defines the global electrophilic nature of a molecule relatively [31]. The molecule with higher ω acts as an electrophile (electron-poor specie) however the molecule with lower ω acts as a nucleophile (electron-rich specie). According to Table 3, it was concluded that CO acted as a nucleophile ($\omega = 0.090$ eV) whereas W acted as an electrophile ($\omega = 0.094$ eV) in OC…W interaction. However, OC…W and W had the same electrophilicity indexes ($\omega = 0.094$ eV) in the formation of OC…2W interaction. Similar to OC…W interaction, OC…2W acted as a nucleophile ($\omega = 0.090$ eV) while W acted as an electrophile ($\omega = 0.094$ eV) in the formation of OC…3W interaction.

Molecules with high HOMO energy can donate their electrons more easily than molecules with low HOMO energy, and therefore they are more reactive in oxidation reactions. Molecules with low LUMO energy are more favored to accept electrons than molecules with high LUMO energy, and as a result they are more reactive in reduction reactions. This approach is used in describing the reactivity (stability) of the molecules [27]. The $f_{H/L}$ index is defined as a stability index of molecules through oxidation. It is the ratio between HOMO and LUMO energies. (Note that $f_{H/L}$ is a unitless index since it is just the ratio of the frontier molecular orbital energies having the same unit.) Molecules with low values of $f_{H/L}$ show persistent character to oxidation than molecules with high values of $f_{H/L}$ [27]. According to this phenomena, it was possible to remark that CO was the most suitable specie for oxidation ($f_{H/L} = -6.75$) whereas W was the least suitable one ($f_{H/L} = -11.86$). The OC…W$_n$ (n = 1-3) species lied in between CO and W in terms of oxidizability (Table 3).

4.   CONCLUSION

The major outcomes of this research can be listed according to the experimental (sensor monitoring) and computational (molecular modeling) studies as follows:
a) Firstly, it would be better to mention that the results all belong to Zonguldak province of Turkey and may differ according to the location.
b) The experimental sensor monitoring and OC…W$_n$ (n = 1-3) computational modeling results correlated well with each other.
c) Temperature and humidity % were found to be the main factors affecting carbon monoxide and humidity interactions.
d) It was concluded that lower temperatures accompanied by higher humidity % were more favored for the interaction of carbon monoxide and humidity since humidity could not be dried sufficiently at lower temperatures.
e) The possible OC…W$_n$ (n=1-3) interactions were examined theoretically within the limitation of the method and basis set used. However the computational results may differ according to these parameters, a post Hartree-Fock

method of MP2 with 6-311++G(d,p) basis set allowed to make relative comparisons. On the other hand, the low-cost components of the experimental setup are generally used in research and developing prototypes. If they were replaced with the industrial versions in the present study, the results would be more improved.
f) The possible sources of error can be listed as follows: using low-cost sensors, sensor noise, the magnitude and direction of the wind (since the data was collected in open air), using a microprocessor with 10-bits analog to digital converter (ADC) (higher than 10-bits ADC would give better results).
g) The future work may include higher level theoretical calculations accompanied by data collections in more days of the year.
h) The CO-humidity modeling proposed in the present study may be integrated into next-generation CO sensors so as to improve the accuracy and precision output. Appropriate chemical desiccants put in the sensor systems may prevent the effect of humidity and support the validity of the proposed chemical model.

REFERENCES

[1] P. Wei, Z. Ning, S. Ye, L. Sun, F. Yang, K.C. Wong, D. Westerdahl and P.K.K. Louie, "Impact analysis of temperature and humidity conditions on electrochemical sensor response in ambient air quality monitoring," Sensors, vol. 18, no 2, pp. 59, Feb. 2018.
[2] W. Yi, K. Lo, T. Mak, K. Leung, Y. Leung and M.A. Meng, "Survey of wireless sensor network based air pollution monitoring systems," Sensors, vol. 15, no 12, pp. 31392-31427, Dec. 2015.
[3] W. Jiao, G. Hagler, R. Williams, R. Sharpe, R. Brown, D. Garver, R. Judge, M. Caudill, J. Rickard, M. Davis, L. Weinstock, S. Zimmer-Dauphinee and K. Buckley, "Community air sensor network (CAIRSENSE) project: evaluation of low-cost sensor performance in a suburban environment in the southeastern United States," Atmos. Meas. Tech., vol. 9, no 11, pp. 5281-5292, Nov. 2016.
[4] L. Spinelle, M. Gerboles, M.G. Villani, M. Aleixandre and F. Bonavitacola, "Field calibration of a cluster of low-cost commercially available sensors for air quality monitoring. Part B: NO, CO and CO_2," Sens. Actuators, B, vol. 238, pp. 706-715, Jan. 2017.
[5] M. Aleixandre and M. Gerboles, "Review of small commercial sensors for indicative monitoring of ambient gas," Chem. Eng. Trans., vol. 30, pp. 169-174, Sep. 2012.
[6] G. Whitenett, G. Stewart, K. Atherton, B. Culshaw and W. Johnstone, "Optical fibre instrumentation for environmental monitoring applications," J. Opt. A: Pure Appl. Opt., vol. 5, no 5, pp. S140-S145, Sep. 2003.

[7] G.F. Fine, L.M. Cavanagh, A. Afonja and R. Binions, "Metal oxide semi-conductor gas sensors in environmental monitoring," Sensors, vol. 10, no 6, pp. 5469-5502, Jun. 2010.

[8] M.I. Mead, O.A.M. Popoola, G.B. Stewart, P. Landshoff, M. Calleja, M. Hayes, J.J. Baldovi, M.W. McLeod, T.F. Hodgson, J. Dicks, A. Lewis, J. Cohen, R. Baron, J.R. Saffell and R.L. Jones, "The use of electrochemical sensors for monitoring urban air quality in low-cost, high-density networks," Atmos. Environ., vol. 70, pp. 186-203, May 2013.

[9] C. Lin, J. Gillespie, M.D. Schuder, W. Duberstein, I.J. Beverland and M.R. Heal, "Evaluation and calibration of Aeroqual series 500 portable gas sensors for accurate measurement of ambient ozone and nitrogen dioxide," Atmos. Environ., vol. 100, pp. 111-116, Jan. 2015.

[10] L. Spinelle, M. Gerboles, M.G. Villani, M. Aleixandre and F. Bonavitacola, "Field calibration of a cluster of low-cost available sensors for air quality monitoring. Part A: Ozone and nitrogen dioxide," Sens. Actuators, B, vol. 215, pp. 249-257, Aug. 2015.

[11] J. A. Streeton, "A Health Data on Review of Existing Six Pollutants" NEPC Service Corporation, Adelaide, SA, Australia, ISBN 0 642 323 29 1, (2000).

[12] H. Dubost and L. Abouaf-Marguin, "Infrared spectra of carbon monoxide trapped in solid argon. Double-doping experiments with H2O, NH3 and N2," Chem. Phys. Lett., vol. 17, no 2, pp. 269-273, Nov. 1972.

[13] D. Yaron, K.I. Peterson, D. Zolandz, W. Klemperer, F.J. Lovas and R.D. Suenram, "Water hydrogen bonding: the structure of the water-carbon monoxide complex," J. Chem. Phys., vol. 92, no 12, pp. 7095-7109, Jun. 1990.

[14] J. Sadlej and V. Buch, "*Ab initio* study of the intermolecular potential of the water-carbon monoxide complex," J. Chem. Phys., vol. 100, no. 6, pp. 4272-4283, Mar. 1994.

[15] J. Lundell and Z. Latajka, "Density functional study of hydrogen-bonded systems: the water-carbon monoxide complex," J. Phys. Chem. A, vol. 101, no 27, pp. 5004-5009, Jul. 1997.

[16] J.J.P. Stewart, "Optimization of parameters for semiempirical methods. I Method," J. Comput. Chem., vol. 10, no 2, pp. 209-220, Mar. 1989.

[17] D. C. Young, Computational Chemistry, New York: Wiley, 2001.

[18] A. Ebrahimi, P. Karimi, F.B. Akher, R. Behazin and N. Mostafavi, "Investigation of the π-π stacking interactions without direct electrostatic effects of substituents: the aromatic‖aromatic and aromatic‖anti-aromatic complexes," Mol. Phys., vol. 112, no 7, pp. 1047-1056, 2014 (Published online: Sep. 2013).

[19] S.K. Mudedla, K. Balamurugan and V. Subramanian, "Computational study on the interaction of modified nucleobases with graphene and doped graphenes," J. Phys. Chem. C, vol. 118, no 29, pp. 16165-16174, Jul. 2014.

[20] S.F. Boys and F. Bernardi, "The calculation of small molecular interactions by the differences of separate total

energies. Some procedures with reduced errors," Mol. Phys., vol. 19, no 4, pp. 553-566, 1970 (Published online: Aug. 2006).

[21] J.D. Mottishaw and H. Sun, "Effects of aromatic trifluoromethylation, fluorination, and methylation on intermolecular π-π interactions," J. Phys. Chem. A, vol. 117, no 33, pp. 7970-7979, Aug. 2013.

[22] M. J. Frisch, G. W. Trucks, H. B. Schlegel, G. E. Scuseria, M. A. Robb, J. R. Cheeseman, G. Scalmani, V. Barone, B. Mennucci, G. A. Petersson, H. Nakatsuji, M. Caricato, X. Li, H. P. Hratchian, A. F. Izmaylov, J. Bloino, G. Zheng, J. L. Sonnenberg, M. Hada, M. Ehara, K. Toyota, R. Fukuda, J. Hasegawa, M. Ishida, T. Nakajima, Y. Honda, O. Kitao, H. Nakai, T. Vreven, J. A. Montgomery Jr., J. E. Peralta, F. Ogliaro, M. Bearpark, J. J. Heyd, E. Brothers, K. N. Kudin, V. N. Staroverov, R. Kobayashi, J. Normand, K. Raghavachari, A. Rendell, J. C. Burant, S. S. Iyengar, J. Tomasi, M. Cossi, N. Rega, J. M. Millam, M. Klene, J. E. Knox, J. B. Cross, V. Bakken, C. Adamo, J. Jaramillo, R. Gomperts, R. E. Stratmann, O. Yazyev, A. J. Austin, R. Cammi, C. Pomelli, J. W. Ochterski, R. L. Martin, K. Morokuma, V. G. Zakrzewski, G. A. Voth, P. Salvador, J. J. Dannenberg, S. Dapprich, A. D. Daniels, O. Farkas, J. B. Foresman, J. V. Ortiz, J. Cioslowski, and D. J. Fox, Gaussian 09, Revision E.01. (2009). Gaussian Inc., Wallingford CT, USA.

[23] R. G. Pearson, Chemical Hardness: Applications from Molecules to Solids, Weinheim: Wiley, 1997.

[24] P.P. Singh, H.K. Srivastava and F.A. Pasha, "DFT-based QSAR study of testosterone and its derivatives," Bioorg. Med. Chem., vol. 12, no 1, pp. 171-177, Jan. 2004.

[25] H.K. Srivastava, F.A. Pasha, S.K. Mishra and P.P. Singh, "Novel applications of atomic softness and QSAR study of testosterone derivatives," Med. Chem. Res., vol. 18, no 6, pp. 455-466, Jul. 2009.

[26] R.G. Parr, L.v. Szentpály and S. Liu, "Electrophilicity index," J. Am. Chem. Soc., vol. 121, no 9, pp. 1922-1924, Mar. 1999.

[27] E.V. Rokhina and R.P.S. Suri, "Application of density functional theory (DFT) to study the properties and degradation of natural estrogen hormones with chemical oxidizers," Sci. Total Environ., vol. 417-418, pp. 280-290, Feb. 2012.

[28] T. Koopmans, "Über die Zuordnung von Wellenfunktionen und Eigenwerten zu den Einzelnen Elektronen Eines Atoms," Physica, vol. 1, no 1-6, pp. 104-113, 1934.

[29] I. Fleming, Frontier Orbitals and Organic Chemical Reactions, London: Wiley, 1976.

[30] J. E. Huheey, Inorganic Chemistry: Principles of Structure and Reactivity, New York: Harper & Row Pub., 1978.

[31] A. Raya, C. Barrientos-Salcedo, C. Rubio-Póo and C. Soriano-Correa, "Electronic structure evaluation through quantum chemical descriptors of 17β-aminoestrogens with an anticoagulant effect," Eur. J. Med. Chem., vol. 46, no 6, pp. 2463-2468, Jun. 2011.